BIOCHEMISTRY

 Volume 44, Number 48 December 6, 2005

Accelerated Publications

Enzyme Function of the Globin Dehaloperoxidase from *Amphitrite ornata* Is Activated by Substrate Binding†

Jennifer Belyea,‡ Lauren B. Gilvey,‡ Michael F. Davis,‡ Marisha Godek,‡,# Tim L. Sit,§ Steven A. Lommel,§ and Stefan Franzen*,‡

Department of Chemistry and Department of Plant Pathology, North Carolina State University, Raleigh, North Carolina 27695

Received August 27, 2005; Revised Manuscript Received October 16, 2005

ABSTRACT: *Amphitrite ornata* dehaloperoxidase (DHP) is a heme enzyme with a globin structure, which is capable of oxidizing para-halogenated phenols to the corresponding quinones. Cloning, high-level expression, and purification of recombinant DHP are described. Recombinant DHP was assayed by stopped-flow experiments for its ability to oxidatively debrominate 2,4,6-tribromophenol (TBP). The enzymatic activity of the ferric form of recombinant DHP is intermediate between that of a typical peroxidase (horseradish peroxidase) and a typical globin (horse heart myoglobin). The present study shows that, unlike other known peroxidases, DHP activity requires the addition of substrate, TBP, prior to the cosubstrate, peroxide. The presence of a substrate-binding site in DHP is consistent with a two-electron oxidation mechanism and an obligatory order for activation of the enzyme by addition of the substrate prior to the cosubstrate.

A globin isolated from the terebellid polychaete *Amphitrite ornata* was reported to have peroxidase activity (*1*). Dehaloperoxidase (DHP)[1] has been shown to debrominate 2,4,6-tribromophenol (TBP) in the presence of peroxide (*1*) (eq 1).

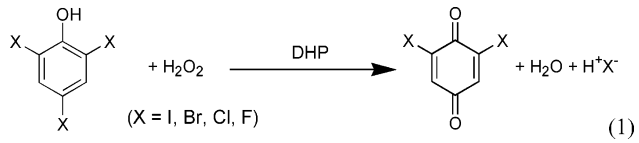

(1)

DHP is classified as a globin (*2*) based on the X-ray crystal structure (*3*, *4*), which resolved eight α-helices arranged in a fold that resembles myoglobins and hemoglobins. However, unlike any known globin, DHP also binds a substrate as proven by an X-ray structure with a substrate analogue (4-iodophenol), which was observed in a well-defined binding site above the heme (*3*, *4*). The exact nature of the product distribution of DHP has not been determined, but enzymatic assays have suggested that the reactivity of DHP is similar to that of horseradish peroxidase (HRP) (*5*−*7*). Peroxidase activity is indicative of a unique mechanism for DHP since there is no structural, sequence, or phylogenetic relationship between DHP and any known peroxidase.

The hypothesis that DHP is a peroxidase implies a ferric (Fe^{3+}) resting state. However, a ferric iron appears to be in contradiction with the role of DHP as a globin or oxygen

† This project was supported by NSF Grant MCB-9874895.

* To whom correspondence should be addressed. Telephone: (919) 515-8915. Fax: (919) 515-8920. E-mail: Stefan_Franzen@ncsu.edu.
‡ Department of Chemistry.
§ Department of Plant Pathology.
# Present address: Dept. of Chemistry, Colorado State University, Fort Collins, CO 80523.

[1] Abbreviations: CcP, cytochrome *c* peroxidase; DHP, dehaloperoxidase; Hb, hemoglobin; HRP, horseradish peroxidase; HHMb, horse heart myoglobin; Mb, myoglobin; SDS−PAGE, sodium dodecyl sulfate−polyacrylamide gel electrophoresis; TBP, 2,4,6-tribromophenol.

10.1021/bi051731k CCC: $30.25
Published on Web 11/09/2005

transport protein, which must have a ferrous (Fe^{2+}) resting state. The structural similarity of DHP with the globin family, its ability to bind oxygen, and the relative abundance of DHP in *A. ornata* suggest that DHP has the function of both a globin and a dehaloperoxidase. However, DHP lacks almost all of the structural features observed in peroxidases. The proximal histidine of DHP is not hydrogen bonded to an aspartate (*3*, *8*−*10*) but rather to the carbonyl group of Leu83. Resonance Raman spectroscopy indicates that the hydrogen bonding of the proximal histidine in DHP to the backbone carbonyl is stronger than that of myoglobin (Mb) or hemoglobin (Hb) (*11*, *12*) but weaker than that of HRP (*13*, *14*). Theoretical studies suggest that this strong hydrogen bonding should help to support formation of compound I (*15*). The heme is shifted relative to the α-helices of the globin so that the closest residue is Val59 (which corresponds to Val68 in sperm whale Mb) rather than the histidine found in all known peroxidases and globins. Moreover, DHP has low sequence homology with most globins and does not resemble engineered myoglobins that have peroxidase function (*16*).

The oxidation of trihalophenols by HRP is presumed to occur by a mechanism involving two one-electron processes mediated by the heme intermediates, compounds I and II (*5*). Compound I is formed from bound peroxide [heme-Fe(III)-H-O-O-H] with a catalytic role played by the distal histidine and a nearby distal arginine. The structure of these residues supports proton transfer to yield the transient species [heme-Fe(III)-O−OH_2], which undergoes heterolytic cleavage resulting in a formal 4+ state of the heme iron heme cation radical [$heme^+$-Fe(IV)═O + H_2O] known as compound I. The mechanism has been studied in detail (*17*, *18*) and is observed in all peroxidases that have been studied (*10*, *19*, *20*). While a histidine (His55) exists in the DHP structure, it is observed in two conformations, only one of which is in the distal pocket (*3*, *4*). The present study shows a significant functional difference between DHP and peroxidases. If cosubstrate H_2O_2 is added to the DHP enzyme before the substrate, TBP, there is no activity. H_2O_2 can act as a suicide inhibitor of HRP (*21*), but this is a different mode of inhibition than that observed for DHP. The inhibition in DHP is hypothesized to arise from the fact that DHP requires a two-electron mechanism, while HRP and most other peroxidases function using a one-electron mechanism. The functional difference is hypothesized to arise from the requirement for two-electron oxidation of the substrate bound in an internal pocket in DHP (*3*, *4*), whereas HRP acts on substrates at the heme edge by a one-electron oxidation mechanism (*22*).

DHP is coded by two genes (*dhpA* and *dhpB*) that have a similar sequence and are likely functional homologues (*23*). In the present study, it is shown that a high-yield expression of DHP using the native *dhpA* gene (*24*) is not possible due to the presence of four eukaryotic AGG (arginine) codons that severely restricts protein expression in *Escherichia coli* (*25*−*27*). In particular, the presence of two consecutive AGG codons in the gene results in variable expression depending on the *E. coli* strain. The cloning and expression of DHP in three *E. coli* strains [TB1, BL21(DE3), and Rosetta(DE3)-pLysS] is discussed. Usable quantities of pure protein are obtained only from an *E. coli* strain containing additional tRNAs for rare codons [Rosetta(DE3)pLysS] or when at least two of the AGG codons have been mutated to the more common prokaryotic CGC codon for arginine.

MATERIALS AND METHODS

Cloning DHP into the pET-16b Expression Vector. The DHP coding region was amplified from a cDNA construct (*23*) with PfuTurbo DNA polymerase (Stratagene, La Jolla, CA) using primers DHP-5′ and DHP-3′ (see Supporting Information) that incorporated a unique *Nco*I site at the amino terminus and a *Bam*HI site at the carboxyl terminus, respectively. An alternate 5′ primer coding for an additional six amino terminal histidine residues (6XHis-DHP) was also used to produce a 5′ histidine-tagged DHP for ease of purification on Ni−NTA columns. The amplified DNA fragments were double digested with *Nco*I/*Bam*HI (New England Biolabs, Beverly, MA) and ligated into similarly cleaved pET-16b (Novagen, Madison, WI) followed by transformation into *E. coli* DH5α. Clones were screened by restriction analysis and sequenced to ensure faithful amplification of the DHP coding region. The resultant constructs were named pET-DHP and pET-6XHisDHP for the native and 6XHis-tagged DHP, respectively.

Mutagenesis of DHP AGG Codons. As an alternative strategy to increase the expression of DHP in *E. coli*, the four Arg codons (R14, R32, R33, and R122) were mutated from AGG to CGC (see Supporting Information for sequence data and primers). The first construct involved mutagenesis of the adjacent AGG codons R32 and R33 simultaneously using a single mutagenic primer (DHP-R32/33). This produced construct pET-DHP2R, which was subsequently used as the template for the simultaneous mutagenesis of residues R14 and R122 with separate primers (DHP-R14 and DHP-R122) to yield construct pET-DHP4R. The mutagenesis reactions were performed using the QuikChange Multi Site-Directed Mutagenesis kit (Stratagene). DNA was purified from transformants using the QIAprep Spin Miniprep kit (Qiagen, Valencia, CA). All mutations were verified by sequence analysis.

Expression of DHP/6XHisDHP in Rosetta(DE3)pLysS and BL21(DE3) Cells. Plasmids pET-DHP, pET-DHP2R, pET-DHP4R, and pET-6XHisDHP were transformed into Rosetta-(DE3)pLysS (Novagen, Madison, WI) and BL21(DE3) cells and plated onto 2XYT agar plates containing the appropriate antibiotics. Flasks containing 2XYT media with the appropriate antibiotics were inoculated with bacteria and incubated at 37 °C with shaking for 2 h. DHP expression was induced by the addition of IPTG to a final concentration of 1 mM followed by incubation for an additional 2 h. The cultures were pelleted and stored at −20 °C prior to DHP extraction.

Purification of DHP from Rosetta(DE3)pLysS and BL21-(DE3) Cells. A 50 g cell pellet was thawed and resuspended by stirring in 200 mL of lysis buffer (50 mM Tris-HCl pH 8, 100 mM NaCl, 5 mM EDTA) for 30 min at 4 °C. The cell suspension was then subjected to a rapid freeze−thaw cycle with liquid nitrogen followed by incubation at 37 °C. The cell slurry was pelleted at 26900*g* for 20 min. The resultant supernatant and pellet were collected separately. When expression yields were high, the presence of DHP was evident from the reddish-brown color of the supernatant.

Heme biosynthesis was anticipated to lag behind the synthesis of the protein; thus, heme was added to the lysis

solution that contained apo-protein to maximize the yield. The pellet was resuspended in 100 mL of lysis buffer containing 40 μL of heme solution (10 mg heme/mL in 0.1 M NaOH) per gram of original cell pellet and stirred for 30 min at 4 °C. The cells were then disrupted with a Fisher Scientific FS20 sonicator for 30 min followed by centrifugation for 25 min at 26900*g*. The supernatant was collected, 0.5 mL of heme solution was added, and the mixture was incubated at 4 °C for 1 h with stirring. This mixture was then centrifuged for 15 min at 26900*g*. The supernatants from all of the steps were combined and dialyzed against three changes of column buffer (20 mM Na phosphate pH 5) until the pH of the column buffer remained at 5.0 (~12 h total). Following dialysis, the crude DHP solution was centrifuged for 15 min at 26900*g*, and the supernatant was collected.

DHP was further purified using CM52 cation exchange cellulose (Whatman, Clifton, NJ) in a 55 mL FLEX-COLUMN (Kimble/Kontes, Vineland, NJ). Approximately 40 mL of resin was equilibrated with 3.5 L of column buffer. The reddish-brown protein solution was loaded onto the equilibrated column and was washed with 80 mL of column buffer. A 300 mL linear gradient from salt-free to 0.5 M NaCl in 20 mM sodium phosphate pH 5 was used to elute the protein. Fractions were collected and analyzed for DHP using a Hewlett-Packard 8453 UV−Vis spectrophotometer. DHP purity was calculated as the ratio of $A_{414\ nm}/A_{280\ nm}$. All fractions with a purity number of 2.5 or greater were pooled and concentrated with an Amicon Centriprep YM-10 unit (Millipore, Billerica, MA). The concentrated protein solution was then loaded onto an 80 mL Sephacryl S-300 column (Sigma-Aldrich, St. Louis, MO) in 20 mM sodium phosphate pH 5 buffer. Fractions from this column were analyzed by SDS−PAGE.

The addition of hemin to the protein to constitute apo-DHP (vide supra) results in mixed oxidation states of the heme. To ensure that only the ferric form was isolated, the DHP protein was treated with 1.7 molar excess of potassium ferricyanide (Fisher Scientific, Hampton, NH) at room temperature. Excess ferricyanide was removed by allowing the sample to flow through a Sephadex G-25 column by gravity. The protein was concentrated using an Amicon Centriprep YM-10 unit, and the purity of the DHP was determined as mentioned previously. Purity numbers in this case were always greater than 3.4. The concentration of the DHP was determined spectrophotometrically at 414 nm using a molar absorptivity of $1.88 \times 10^5\ M^{-1}\ cm^{-1}$.

Purification of 6XHisDHP from Rosetta(DE3)pLysS Cells. A 50 g cell pellet was allowed to thaw in 500 mL of lysis buffer (50 mM NaH_2PO_4, 300 mM NaCl, 10 mM imidazole, pH 8) for 15 min followed by stirring at 4 °C for 10 min. Lysozyme was added to the cell slurry to a final concentration of 1 mg/mL, and the mixture was incubated on ice for 30 min. Subsequently, the cell mixture was sonicated as mentioned above for 30 min in an ice water bath. RNase A and DNase I were added to the viscous lysate to final concentrations of 60 and 19 μg/mL, respectively. The mixture was incubated on ice for 15 min before centrifugation at 10000*g* for 30 min at 4 °C.

The 6XHis-DHP was purified with Ni-NTA agarose columns (Qiagen) following a modified procedure from the manufacturer. The translucent red lysate was loaded onto the column, followed by the addition of 3 column volumes of wash buffer (50 mM NaH_2PO_4, 300 mM NaCl, 20 mM imidazole, pH 8). The 6XHis-DHP was eluted off the column by the addition of 50 mL elution buffer (50 mM NaH_2PO_4, 300 mM NaCl, 250 mM imidazole, pH 8). Fractions were collected according to the intensity of the color of the eluted protein solution. Once the column was completely eluted the fractions were analyzed by SDS−PAGE and by UV−vis spectroscopy. Fractions that had a purity number of 2.5 or greater were pooled and concentrated.

Table 1: Analysis of DHP Yields from Various Expression Vectors and *Escherichia coli* Strains

construct	*E. coli* strain	DHP (mg/g of cell pellet)[a]
pUC-DHP	TB1	0.2
pUC-DHP	BL21(DE3)	~0
pET-DHP	BL21(DE3)	~0
pET-DHP	Rosetta(DE3)pLysS	4.2
pET-DHP2R	BL21(DE3)	5.1
pET-DHP2R	Rosetta(DE3)pLysS	4.0
pET-DHP4R	BL21(DE3)	7.5
pET-DHP4R	Rosetta(DE3)pLysS	4.2

[a] The yield of DHP protein is reported for different combinations of expression vector and *E. coli* strain.

Growth Studies. Protein production comparisons between pUC19-DHP (*24*) in *E. coli* TB1 and pET-DHP in either *E. coli* BL21(DE3) or Rosetta(DE3)pLysS were performed by two methods. The growth and expression of vector/*E. coli* strain combinations (see Table 1) were performed according to the published protocol for the growth and expression of DHP from pUC19-DHP in TB1 cells (*24*). Protein production levels were assessed by electrophoresis in 15% SDS−polyacrylamide gels. Gels were stained with Bio-Safe Coomassie Stain (Bio-Rad, Hercules, CA) according to the manufacturer's specifications.

Assays for Peroxidase Activity. UV−Vis spectroscopy and stopped-flow experiments were used to assay for peroxidase activity on the native substrate, TBP. The solutions of TBP were made in an amber bottle and kept in an ice water bath immediately prior to a day's experiments and kept for no more than 4 h. Isolation from light and cold temperature storage were necessary to avoid degradation of the TBP. Stopped flow measurements were performed on an Applied Photophysics SX.18MV Stopped-flow Reaction analyzer (Surrey, UK) at constant pressure using excess TBP to maintain pseudo-first-order conditions. For each set of reaction conditions, 25−30 replicates were performed. The progress of the reactions was monitored at 272 nm for the appearance of products and at 316 nm for the decrease in substrate concentration. The results from multiple measurements of each reaction were averaged and fit to an exponential function to determine the rate constant. Constant temperature was obtained by a circulating water bath at 20 °C, and constant pressure was maintained with nitrogen gas.

RESULTS AND DISCUSSION

Expression of Native DHP in E. coli. It was recently reported that the *dhpA* gene from *A. ornata* cloned into pUC19 could be expressed in *E. coli* TB1 for recombinant protein purification (*24*). After obtaining this same construct, a yield of ~0.2 mg/g of cell pellet was obtained using the reported protocol (Table 1). The cell pellets obtained from TB1 with the pUC19 plasmid are a faint orange color.

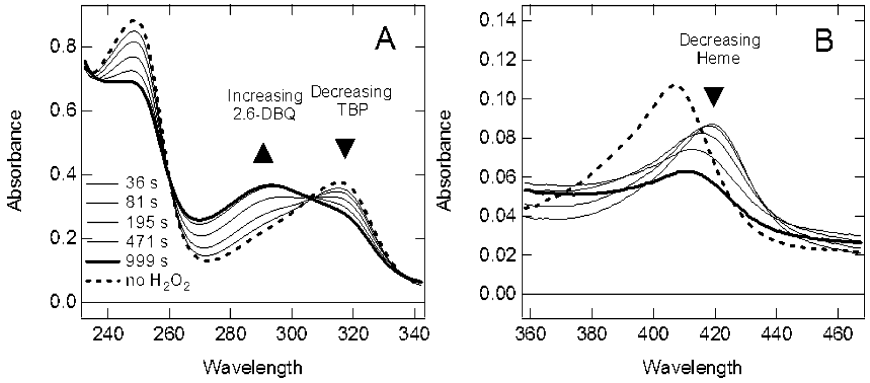

FIGURE 1: (A, B) UV−visible absorption spectrum of DHP reaction with substrate 2,4,6-tribromophenol (TBP). Assay conditions 0.5 μM enzyme, 125 μM peroxide, 100 μM TBP, and 10 mM KP buffer pH 7. The time delays are given in seconds. The dotted line indicates the spectrum of DHP and TBP without added H_2O_2.

Normally, overexpression of heme proteins leads to a reddish-brown cell pellet even when heme biosynthesis is less rapid than protein expression. Perhaps more importantly, the protein produced from the pUC-DHP construct in *E. coli* TB1 cells was difficult to purify, and even after gel filtration and ion exchange columns there appeared to be multiple protein products that were resolved by gel electrophoresis. In repeated expression tests of the pUC-DHP plasmid, it was not possible to isolate a usable quantity of DHP protein from TB1 cells.

To increase the yield of DHP from *E. coli*, the DHP gene was subcloned into the high-level expression vector pET-16b. Construct pET-DHP was transformed into BL21(DE3) cells, and DHP expression was induced. However, no detectable DHP production was observed (Table 1). We hypothesized that this failure was due to the presence of four AGG (arginine) codons in the DHP gene. The AGG codon is one of the least commonly used in *E. coli* and is known to lead to stalled protein expression and frameshift mutations (*25*−*27*). One remedy for this problem was to transform the pET-DHP native sequence construct into Rosetta(DE3)pLysS cells. This strain contains a plasmid that encodes rare *E. coli* tRNAs to permit protein expression from genes that contain low frequency codons. As anticipated, DHP synthesis from pET-DHP was observable in the Rosetta strain. In fact, the combination of pET-DHP/Rosetta(DE3)pLysS cells significantly improved the yield of DHP by 20-fold over that observed for pUC-DHP/TB1 cells (Table 1). Moreover, the protein produced in Rosetta(DE3)pLysS cells could be purified as a single species.

Expression of Modified DHP in E. coli. While usable quantities of protein could be obtained with pET-DHP/Rosetta(DE3)pLysS, the resulting yields were still less than optimum under the pET system due to the slow growth habit of the Rosetta cells. Mutation of the AGG codons in the *dhpA* gene of DHP was performed to test the hypothesis that the lack of protein production from pET-DHP in BL21(DE3) cells was attributable to the four occurrences of the AGG codon in the *dhpA* gene. Plasmids were produced that contained the silent mutation AGG → CGC. The mutagenesis was performed in two stages. First, the consecutive AGG codons at positions R32/R33 in the DHP sequence were considered. Successful mutagenesis of these two codons to CGC (pET-DHP2R) increased the expression of DHP to ∼5 mg/g of cell pellet in BL21(DE3) cells. DHP expression in BL21(DE3) cells was optimal when all four AGG codons

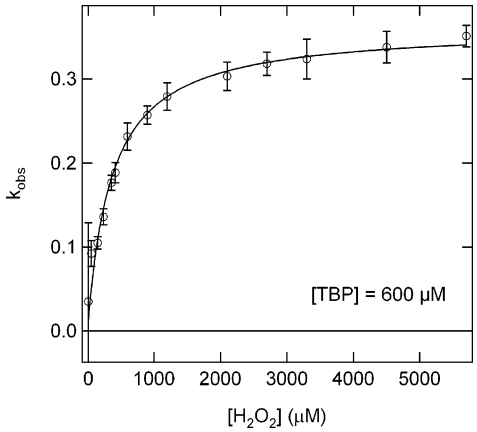

FIGURE 2: Stopped-flow data for DHP activity as a function of hydrogen peroxide concentration. Assay conditions were 6 μM His-DHP, 0.05 M KNO_3, 600 μM TBP, 10 mM KP buffer pH 6 and H_2O_2 concentrations between 0 and 5500 μM. The observed rate constant was obtained from single-exponential fits to the stopped-flow data. The fitting function used was $k_0 = k_{obs}[H_2O_2]/(K_M + [H_2O_2])$ and the parameters obtained were $k_{obs} = 0.36 \pm 0.03$ s^{-1} and $K_M = 356 \pm 37$ μM. $V_{max} = 10.8 \pm 0.9$ μmol of product s^{-1} is obtained by multiplying the observed maximum rate constant k_{obs} by the concentration of product formed $[O{=}A{=}O]_{final} \sim 30$ μM. This value was obtained from the $\Delta A \sim 0.042$ divided by the extinction coefficient of 14 000 M^{-1} cm^{-1} and the path length of 0.1 cm.

(R14, R32/R33, and R122) were mutated to CGC (pET-DHP4R) leading to yields of 7.5 mg/g of cell pellet (Table 1). Table 1 provides strong evidence that the presence of two consecutive AGG codons has a particularly strong negative effect on protein expression in *E. coli*.

Assays for Enzymatic Activities of Recombinant DHP. Functional assays for the enzyme activity of recombinant DHP were carried out using both a photodiode array spectrometer (Figure 1) and stopped-flow measurements (Figures 2 and 3). A photodiode array spectrometer was used for manual mixing experiments with a time resolution of roughly 1 s. Figure 1A shows that substrate absorption bands (316 nm) decrease in intensity and product absorption bands (272 nm) increase in intensity. Figure 1B shows that the Soret band of the heme is observed to shift from 409 nm (ferric DHP) to 420 nm (compound II). There was no evidence of a compound I species with this time resolution.

Comparisons of 6XHis-DHP with HRP and horse heart myoglobin (HHMb) were carried out using stopped-flow experiments. As seen in Figure 3, the observed rate constants

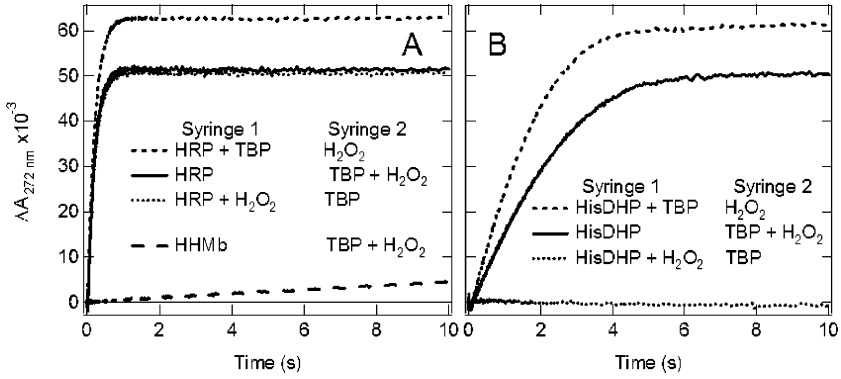

FIGURE 3: Stopped-Flow absorption data monitored at 272 nm assay the formation of product 2,6-dibromoquinone. The contents of each syringe used in the stopped-flow experiment are given in the figure legend. Assay conditions were 6 μM respective enzyme, 0.05 M KNO_3, 650 μM H_2O_2, 600 μM TBP, and 10 mM KP buffer pH 5. (A) The control experiments for HRP are shown for three different configurations of the mixing syringes. A control experiment for HHMb is shown as the bottom trace in the figure. (B) The rise of product formation for DHP is shown for three configurations of the mixing syringes. The dotted line at the bottom represents the case in which H_2O_2 is premixed with DHP. The baseline is omitted for clarity in this panel.

have the order HRP > 6XHis-DHP > HHMb. The turnover numbers [μmol of products (μmol of enzyme)$^{-1}$ s^{-1}] are 25.9 $\pm$ 1.8, 2.0 $\pm$ 0.28, and 0.17 $\pm$ 0.02 under these conditions when comparing the rate of product formation at 272 nm and pH = 5. Similar results were obtained at pH 6 and pH 7 (see Supporting Information). Furthermore, the kinetics of 6XHis-DHP and DHP were observed to be nearly identical (see Supporting Information).

The results of peroxide activation studies for 6XHis-DHP shown in Figure 2 give the expected hyperbolic dependence of the rate constant on [H_2O_2] and can be fit to a functional form that resembles the Michaelis−Menten equation: $V_0 = V_{max}[H_2O_2]/(K_P + [H_2O_2])$. K_P represents a Michaelis constant for the cosubstrate H_2O_2. In this interpretation of the stopped-flow data, the turnover was $k_{cat} = 1.8 \pm 0.15$ μmol of product (μmol of enzyme)$^{-1}$ s^{-1}, which lead to an effective $V_{max} = k_{cat}[E] = 10.8 \pm 0.9$ μM product/s and an effective Michaelis constant for cosubstrate of $K_P \sim 356 \pm 37$ μM^{-1} at pH 6. The extinction coefficient of TBP is 14 000 M^{-1} s^{-1} at 270 nm. The maximum observed ΔA of ~0.04 in a path length of 0.1 corresponds to ~5% conversion of substrate to product and indicated that a maximum of five turnovers occur during the stopped-flow experiment.

Interpretation of the data differs from a true Michaelis−Menten analysis in two important ways. First, H_2O_2 is not the substrate but rather the cosubstrate. One might assume that in the stopped-flow experiment the enzyme−substrate complex in one syringe acts as a single complex and that H_2O_2 binds and reacts in a manner analogous to a substrate. However, the second important difference with respect to Michaelis−Menten conditions is that H_2O_2 in solution is not in equilibrium with iron-bound H_2O_2. These points have been addressed by Dunford in the book *Heme Peroxidases*, in which an alternative analysis to Michaelis−Menten is presented (*28*). According to the kinetic analysis (*28*), the dependence on H_2O_2 and substrate (TBP) must be considered simultaneously. Although the dependence of the rate constant on substrate concentration (see Supporting Information) does not closely follow the expected hyperbolic dependence (*28*), a fit to such a model yields $K_M \sim 6$ μM^{-1}, which corresponds to ~60 times tighter binding of substrate TBP than H_2O_2 by comparison with the K_P above.

Relationship of DHP Stopped-Flow Measurements to Peroxidase Mechanism. Peroxidases perform either two sequential one-electron oxidations SH → S + H$^+$ + e$^-$ or a single two-electron oxidation XA-OH + H_2O → O═A═O + HX + 2H$^+$ + 2e$^-$. On the basis of the spectral evidence, we assume that the latter mechanism is appropriate for DHP. The main difference in the two mechanisms is a factor of 2 that appears for the one-electron mechanism since 2 equiv of product are produced for each mole of H_2O_2 consumed. In the two-electron mechanism, 1 equiv of H_2O_2 is consumed for each mole of product produced. The three steps in the mechanism are presented below:

$$1.\ \text{DHP} + H_2O_2 \rightarrow \text{compound I} + H_2O \qquad (k_1)$$

$$2.\ \text{Compound I} + \text{XA-OH} \rightarrow \text{compound II} + \text{XA-O}^{\bullet} + H^+ \qquad (k_2)$$

$$3.\ \text{Compound II} + \text{XA-O}^{\bullet} + H^+ \rightarrow \text{DHP} + \text{O═A═O} + \text{HX} \qquad (k_3)$$

where the substrate is XA-OH (X, A-OH, and O═A═O represent the para-halogen, substituted phenol, and the corresponding quinone, respectively). Each of these processes is considered to be irreversible. If one assumes that $k_2 \gg k_3$, the reaction velocity is $V_0 = k_1k_3[E][XA\text{-}OH][H_2O_2]/(k_1[H_2O_2] + k_3[XA\text{-}OH])$. At a substrate concentration of [XA-OH] ~ 600 μM one obtains an effective maximum rate $V_{max} = k_3[E][XA\text{-}OH] = 10.8 \pm 0.9$ μM product/s and the effective $K_M = k_3[XA\text{-}OH]/k_1 = 356 \pm 37$ μM obtained from Figure 2. Given the enzyme and substrate concentrations reported above, the intrinsic rate constants are $k_1 \sim 5 \times 10^3$ M^{-1} s^{-1} and $k_3 \sim 3 \times 10^3$ M^{-1} s^{-1} under the given conditions. According to these data, the rate constant for formation of compound I, k_1 is ~2000 times smaller in DHP than in HRP (*28*). This large difference is attributable in part to side reactions such as heme degradation evident in Figure 1. However, it is clear also that the active site of DHP lacks many of the amino acid residues that are known to accelerate formation of compound I in known peroxidases (*3*, *4*).

There is a competing pathway that can occur when the substrate concentration is sufficiently high. If the intermediate

XA-O$^{\bullet}$ escapes from the DHP binding site after step 2 or if an edge pathway for electron transfer [such as exists in other known peroxidases (*22*)] becomes accessible then a polymerization reaction can occur (*29*).

$$X(A-O)_n^{\bullet} + XA\text{-}OH \rightarrow X(A-O)_n\text{-}A=O^{\bullet} + HX$$

This competing pathway produces an insoluble polymeric product. Under conditions in which excess peroxide is used in solution these reactions can occur as well. These competing reactions complicate the interpretation of data obtained on the time scale of many seconds in manual mixing experiments such as those shown in Figure 1 and presented elsewhere (*24*).

Evidence for an Obligatory Binding of Substrate Before Cosubstrate. The foregoing observations establish that DHP has enzyme characteristics of a peroxidase despite structural differences. However, one of the most profound structural differences between DHP and peroxidases is the substrate-binding site in DHP (*3*, *4*). Unlike DHP typical peroxidases oxidize substrates at the edge of heme (*22*). The difference between heme-edge (HRP) and an interior binding pocket (DHP) raises the mechanistic question of the timing of substrate and cosubstrate binding to the enzyme. Figure 3 shows that there is a profound effect produced by the order of mixing TBP and H_2O_2 with DHP, an affect not observed in HRP. The greatest amount of product is formed for both HRP and DHP when the substrate and enzyme are present (premixed) in one syringe and peroxide is added in the second syringe. Figure 3A shows that for HRP there is no difference between having the peroxide in the syringe with the protein or in a separate syringe. Figure 3B shows that peroxide will inhibit the DHP enzyme if it is added before TBP. In the experiments shown here the peroxide is in contact with the protein for a time interval of approximately one minute prior to stopped-flow mixing with the protein. The data in Figure 1 show that while compound II is formed on this time scale, there is relatively little heme degradation on the time scale of one minute. Why should the order of mixing the substrate and cosubstrate have such a large effect? In the standard edge-binding hypothesis (*22*) for substrate electron transfer to heme and the formation of compound I and II independent of substrate (*8*, *10*) there is no obligatory order for the binding events. The stopped-flow data presented here indicate that there is an obligatory order for the entry of the substrate and cosubstrate into the distal pocket of DHP. Our hypothesis is that the substrate must bind prior to peroxide. The corollary is that substrate binding is also the trigger that is responsible for a change from globin to peroxidase-like function. Since DHP is the first globin to have peroxidase function this hypothesis provides a starting point to understand the function switch in a dual function enzyme.

Comparison of Stopped-Flow and Time-Resolved Diode Array Experiments. A previous study of DHP reported that the maximum rate was obtained when the cosubstrate H_2O_2 concentration was approximately 10−20 times greater than the protein concentration (*24*). However, the stopped-flow data show that the maximum rate is reached when the ratio of H_2O_2/DHP is 160:1, and Figure 2 shows that there is a plateau rather than a maximum provided the substrate is added prior to H_2O_2. The difficulty with interpretation of experiments under manual mixing conditions (*24*) is that there are secondary reactions such as polymerization (discussed above), heme degradation such as shown in Figure 1 and in ref *30*. Despite these shortcomings, the data here do support the hypothesis that the heme becomes "trapped" in the compound II form (*24*). DHP is observed to convert the compound II form when H_2O_2 is present. Figure 1 shows that the heme band shifts from ferric DHP (409 nm) to compound II (420 nm) when H_2O_2 is added. Compound I is observed only transiently in stopped-flow spectral measurements (see Supporting Information). Figure 3 shows that the addition of H_2O_2 prior to substrate, which results in a compound II state, inhibits the enzymatic reaction. This comparison indicates a major difference between DHP, which must have an obligatory two-electron oxidation mechanism and peroxidases such as HRP, which catalyze by single-electron oxidation of the substrate.

Structural Comparisons of DHP to the Active Site of Peroxidases. DHP is capable of dehalogenating a wide range of halogenated substrates (*1*). However, DHP lacks the strong hydrogen bond to the proximal histidine that is the hallmark of peroxidases. Cytochrome *c* peroxidase (CcP) has an aspartate (Asp 235) that hydrogen bonds to the N-δ hydrogen of the imidazole of the proximal histidine and polarizes the ligand to the heme iron (*9*). Similar hydrogen-bonding patterns are found in HRP and lignin peroxidase (*19*, *31*). In DHP, the carbonyl group of residue 83 forms a hydrogen bond to the N-δ hydrogen of the proximal histidine (*4*). Density functional theory calculations are consistent with the observation that even strong hydrogen bonding to a backbone carbonyl results in a polarization of the imidazole that is intermediate between the hydrogen bonding to serine in Mb and to aspartate in CcP (*15*, *32*). This is consistent with resonance Raman measurements, which show that the frequency of the Fe−His stretching vibration of DHP is intermediate between those of HHMb and HRP (*33*). Thus, while the structure and spectroscopic observations can be rationalized in terms of bonding, these observations still do not explain the catalytic ability of DHP.

On the basis of the X-ray crystal structure and spectroscopic measurements such as infrared, UV−vis, magnetic circular dichroism, etc., DHP has the appearance of a typical globin (*3*, *13*, *34*). However, the distal pocket of DHP is more hydrophobic than that of typical globins because of the substrate binding site and because the heme is more deeply buried in the globin. Mbs and Hbs from many species have a distal histidine in the ligand-binding (or distal) pocket. The distal histidine can hydrogen bond to diatomic ligands and to peroxide bound to the heme iron. The distal histidine (His55) of DHP was observed in two positions based on the X-ray structure (*3*, *4*). One of the positions of His55 is in the distal pocket and the other is solvent-exposed. His55 is 1.5 Å further from the iron than the corresponding histidine in globins. While it is true that the distal histidine of peroxidases (e.g., CcP) are farther from the heme iron (e.g., Fe···N$_{\epsilon}$ = 5.6 Å in CcP vs 4.5 Å in Mb), peroxidases have other nearby hydrogen-bonding residues (e.g., Arg 5.3 and Trp 4.2 Å in CcP structure 1CCA) (*9*). The distal pocket of DHP lacks the arginine and tryptophan that facilitate proton transfer (*17*). Moreover, His55 is displaced from the distal pocket when substrate is present in DHP raising the question of how this residue can assist in activation of bound peroxide

in such a mechanism in the first place. The stopped-flow data indicate that enzyme function depends on the order of addition of the substrate, TBP and cosubstrate H_2O_2. These observations need to be explored fully as a function of pH and for different mutant DHP proteins to understand the details of the mechanism.

CONCLUSION

We have successfully cloned the DHP gene into the pET-16b vector that permits high level expression of the native sequence in *E. coli* Rosetta(DE3)pLysS cells. No usable protein was obtained from the native DHP sequence in other *E. coli* strains such as TB1 and BL21(DE3). The small amount of protein that was produced from pUC-DHP in TB1 cells is difficult to purify because of multiple protein products. Mutation of the AGG codons in a pET-16b expression vector permits high-level expression of the DHP protein in BL21(DE3) cells (∼7 mg/g of cell pellet). Stopped-flow experiments showed rates for product formation in the order HRP > DHP > HHMb such that HRP is ∼13 times faster than DHP and DHP is at least 12 times faster than HHMb. DHP is truly an enzyme that is capable of oxidizing halophenols to quinone, but it has significant differences with known peroxidases. The distal histidine, His55 in DHP is the only residue capable of performing proton shuttling in the active site, and this amino acid residue is displaced by substrate binding (*3*, *4*). This observation presents a paradox for DHP function: the substrate must apparently bind before peroxide (Figure 3), and yet this binding of substrate removes the very residue (His55) that would catalyze the formation of compound I when peroxide does bind! The data show that peroxide is an inhibitor if it binds to the enzyme before the substrate. This means that the substrate must be the chemical species that activates enzyme function in DHP. Using the successful cloning and expression methods described here, the implications of this mechanism will be pursued using site-directed mutants to address the functional role of the distal and proximal residues.

ACKNOWLEDGMENT

We thank Prof. Clay Clark and Dr. Ruby Chen for assistance with stopped-flow experiments. We thank Prof. Bert Ely and Kaiping Han for providing the pUC19 plasmid containing the *dhpA* gene accession number AF284381.

SUPPORTING INFORMATION AVAILABLE

The sequence of the DHP gene, primer sequences used for mutagenesis, and figures showing the stopped flow kinetics at pH 6 and 7, as a function of substrate concentration and spectral data. This material is available free of charge via the Internet at http://pubs.acs.org.

REFERENCES

1. Chen, Y. P., Woodin, S. A., Lincoln, D. E., and Lovell, C. R. (1996) An unusual dehalogenating peroxidase from the marine terebellid polychaete *Amphitrite ornata*, *J. Biol. Chem. 271*, 4609−4612.
2. Murzin, A. G., Brenner, S. E., Hubbard, T., and Chothia, C. (1995) SCOP: a structural classification of proteins database for the investigation of sequences and structures, *J. Mol. Biol. 247*, 536−540.
3. LaCount, M. W., Zhang, E. L., Chen, Y. P., Han, K. P., Whitton, M. M., Lincoln, D. E., Woodin, S. A., and Lebioda, L. (2000) The crystal structure and amino acid sequence of dehaloperoxidase from *Amphitrite ornata* indicate common ancestry with globins, *J. Biol. Chem. 275*, 18712−18716.
4. Lebioda, L., LaCount, M. W., Zhang, E., Chen, Y. P., Han, K., Whitton, M. M., Lincoln, D. E., and Woodin, S. A. (1999) An enzymatic globin from a marine worm, *Nature 401*, 445−445.
5. Ferrari, R. P., Laurenti, E., and Trotta, F. (1999) Oxidative 4-dechlorination of 2,4,6-trichlorophenol catalyzed by horseradish peroxidase, *J. Biol. Inorg. Chem. 4*, 232−237.
6. Ferrari, R. P., Laurenti, E., Cecchimi, P. I., Gambino, O., and Sondergaard, I. (1995) Spectroscopic investigations on the highly purified lactoperoxidase Fe(III) heme-catalytic site, *J. Inorg. Biochem. 58*, 109−127.
7. Hewson, W. D., and Dunford, H. B. (1976) Oxidation of *p*-cresol by horseradish peroxidase compound I*, *J. Biol. Chem. 251*, 6036−6042.
8. Choudhury, K., Sundaramoorthy, M., Hickman, A., Yonetani, T., Woehl, E., Dunn, M. F., and Poulos, T. L. (1994) Role of the proximal ligand in peroxidase catalysis − crystallographic, kinetic, and spectral studies of cytochrome-*c* peroxidase proximal ligand mutants, *J. Biol. Chem. 269*, 20239−20249.
9. Goodin, D. B., and McRee, D. E. (1993) The Asp-His-Fe triad of cytochrome-*c* peroxidase controls the reduction potential, electronic-structure, and coupling of the tryptophan free-radical to the heme, *Biochemistry 32*, 3313−3324.
10. Bonagura, C. A., Bhaskar, B., Shimizu, H., Li, H. Y., Sundaramoorthy, M., McRee, D. E., Goodin, D. B., and Poulos, T. L. (2003) High-resolution crystal structures and spectroscopy of native and compound I cytochrome *c* peroxidase, *Biochemistry 42*, 5600−5608.
11. Kitagawa, T., Nagai, K., and Tsubaki, M. (1979) Assignment of the Fe−Nϵ (His F8) stretching band in the resonance Raman spectra of deoxy myoglobin, *FEBS Lett. 104*, 376−378.
12. Scott, T. W., Friedman, J. M., and Macdonald, V. W. (1985) Distal and proximal control of ligand reactivity: A transient Raman comparison of COHbA and COHb (Zurich), *J. Am. Chem. Soc. 107*, 3702−3705.
13. Franzen, S., Roach, M. P., Chen, Y. P., Dyer, R. B., Woodruff, W. H., and Dawson, J. H. (1998) The unusual reactivities of *Amphirite ornata* dehaloperoxidase and *Notomastus lobatus* chloroperoxidase do not arise from a histidine imidazolate proximal heme iron ligand, *J. Am. Chem. Soc. 120*, 4658−4661.
14. Spiro, T. G., Smulevich, G., and Su, C. (1990) Probing protein structure and dynamics with resonance Raman spectroscopy: cytochrome *c* peroxidase and hemoglobin, *Biochemistry 29*, 4497−4508.
15. Franzen, S. (2001) Effect of a charge relay on the vibrational frequencies of carbonmonoxy iron porphine adducts: The coupling of changes in axial ligand bond strength and porphine core size, *J. Am. Chem. Soc. 123*, 12578−12589.
16. Witting, P. K., Mauk, A. G., and Lay, P. A. (2002) Role of tyrosine-103 in myoglobin peroxidase activity: Kinetic and steady-state studies on the reaction of wild-type and variant recombinant human myoglobins with H_2O_2, *Biochemistry 41*, 11495−11503.
17. Poulos, T. L., and Kraut, J. (1980) The Stereochemistry of Peroxidase Catalysis, *J. Biol. Chem. 255*, 8199−8205.
18. Hiner, A. N. P., Raven, E. L., Thorneley, R. N. F., Garcia-Canovas, F., and Rodriguez-Lopez, J. N. (2002) Mechanisms of compound I formation in heme peroxidases, *J. Inorg. Biochem. 91*, 27−34.
19. Poulos, T. L., Edwards, S. L., Wariishi, H., and Gold, M. H. (1993) Crystallographic refinement of lignin peroxidase at 2-Angstrom, *J. Biol. Chem. 268*, 4429−4440.
20. Patterson, W. R., Poulos, T. L., and Goodin, D. B. (1995) Identification of a porphyrin pi-cation-radical in ascorbate peroxidase compound-I, *Biochemistry 34*, 4342−4345.
21. Hiner, A. N. P., Hernandezruiz, J., Garciacanovas, F., Smith, A. T., Arnao, M. B., and Acosta, M. (1995) A Comparative study of the inactivation of wild-type, recombinant and 2 mutant horseradish-peroxidase isoenzymes-c by hydrogen-peroxide and m-chloroperoxybenzoic acid, *Eur. J. Biochem. 234*, 506−512.
22. Ator, M. A., and Montellano, O. d. (1987) Protein control of prosthetic heme reactivity. Reaction of substrates with the heme edge of horseradish peroxidase, *J. Biol. Chem. 262*, 1542−1551.

23. Han, K., Woodin, S. A., Lincoln, D. E., Fielman, T. E., and Ely, B. (2001) *Amphitrite ornata*, a marine worm, contains two dehaloperoxidase genes, *Mar. Biotechnol. 3*, 287−292.
24. Osborne, R. L., Taylor, L. O., Han, K. P., Ely, B., and Dawson, J. H. (2004) *Amphitrite ornata* dehaloperoxidase: enhanced activity for the catalytically active globin using MCPBA, *Biochem. Biophys. Res. Commun. 324*, 1194−1198.
25. Chen, G. F. T., and Inouye, M. (1994) Role of the AGA/AGG codons, the rarest codons in global gene expression in *Escherichia coli*, *Genes Dev. 8*, 2641−2652.
26. Sayers, J. R., Price, H. P., Fallon, P. G., and Doenhoff, M. J. (1995) AGA/AGG codon usage in parasites − implications for gene expression in *Escherichia coli*, *Parasitol. Today 11*, 345−346.
27. Bonekamp, F., and Jensen, K. F. (1988) The AGG codon is translated slowly in *Escherichia coli* even at very low expression levels, *Nucleic Acids Res. 16*, 3013−3024.
28. Dunford, H. B. (1999) *Heme Peroxidases*, Wiley-VCH, New York.
29. Ferreira, M. L. (2003) UV/visible study of the reaction of oxidoreductases and model compounds with H_2O_2, *Macromol. Biosci. 3*, 179−188.
30. Chaudhary, C. (2003) MS Thesis in *Chemistry*, North Carolina State University, Raleigh.
31. Green, M. T. (2000) Imidazole-ligated compound I intermediates: The effects of hydrogen bonding, *J. Am. Chem. Soc. 122*, 9495−9499.
32. Smulevich, G., Feis, A., and Howes, B. D. (2005) Fifteen years of Raman spectroscopy of engineered heme containing peroxidases: What have we learned? *Acc. Chem. Res. 38*, 433−440.
33. Roach, M. P., Chen, Y. P., Woodin, S. A., Lincoln, D. E., and Dawson, J. H. (1997) *Notomastus lobatus* chloroperoxidase and *Amphitrite ornata* dehaloperoxidase both contain histidine as their proximal heme iron ligand, *Biochemistry 36*, 2197−2202.
34. Franzen, S. (2002) An electrostatic model for the frequency shifts in the carbonmonoxy stretching band of myoglobin: Correlation of hydrogen bonding and the Stark tuning rate, *J. Am. Chem. Soc. 124*, 13271−13281.

BI051731K